Research Journal of Biological Sciences 4 (6): 637-643, 2009
ISSN: 1815-8846
© Medwell Journals, 2009

Design Analysis and Performance Prediction of the Cardiac Axial Blood Pump

D.H. Hussein, H. Gitano-Briggs and M.Z. Addullah
School of Mechanical Engineering, University of Sains Malaysia,
Pulau Penang, 14300 Nibong Tebal, Malaysia

Abstract: Computational Fluid Dynamics (CFD) has been used for developing and evaluating the performance of a novel design of the Cardiac Axial Blood Pump (CABP). This device could be used as an implantable pump for boosting blood circulation in patients whose hearts are not providing sufficient output. Based on the Berlin Heart configuration the blood pump has been designed for a flow rate of 5 L min^{-1} and 100 mmHg of head pressure. Finite element analysis method has been performed to predict the shear stress, velocity and pressure drop applied on the fluid through the pump and the shear stress on the pump impeller. Furthermore, flow streamlines has been discussed to predict the flow streamlines behavior and the expected stagnation points. The aim of this research is to design an efficient blood pump to support the blood circulatory system and reduce the shear stress and blood hemolysis during transport through the pump. The design simulated at several rotational speeds (5000-7000 rpm) to investigate the relationship between the rotational speeds and shear stress. Results indicate that the rotational speed has a direct correlation with shear stress and pressure drop. On the same stream, we found that at 6500 rpm the pump gives its optimal pressure drop and shear stress.

Key words: High shear stress, blood hemolysis, bio-compatibility, axial blood pump, biofluid engineering, flow streamlines

INTRODUCTION

Heart disease is the number one killer of adults in the Western world (Tetsuzo, 1975; Hussein and Gitano-Briggs, 2008). About 20 million people worldwide suffer annually from Congestive Heart Failure (CHF), about 25% of them in the United State (US) alone. In the US, a distressingly low 2000-2500 donor hearts is only available each year. One possible approach to recover this situation is to use a mechanical tool to boost or to create blood flow in patients suffering from hemodynamic decline that is loss of blood pressure and lower cardiac output. The ultimate ambition of this device can be replace the natural heart, i.e. Total Artificial Heart (TAH), or to assist an ailing heart, i.e. Ventricular Assist Devices (VAD). In either approach, the device can be used to bridge the gap while, waiting for a matching donor heart for transplantation. However, to ease the shortage of donor hearts, making these devices suitable for long-term or permanent use would be an ultimate aim. Another benefit of an assisted device is the potential for providing time for the natural heart to recover. In some patients, it has been observed that the natural heart can be recovered by unloading the pumping requirement through the use of a VAD (Hafez, 2003). The high demand for qualified and bio-compatible artificial circulatory support systems for temporary support or permanent replace an irreparably human heart is well established. This need became apparent to cardiac surgeons in the early 1950s after the clinical application of the first heart lung machine. Due to a shortage of donor hearts for transplants, the demand for artificial heart pumps has led to worldwide investigation and development of mechanical assisted devices including pneumatic pumps, axial flow pumps and centrifugal pumps. Axial flow pumps, with the advantages of small volume, high efficiency and light weight are widely used as VAD systems (Noon *et al*., 2000). Some VAD's are intended for short term use, typically for patients recovering from heart attacks or heart surgery, while, others are intended for long term use months to years and in some cases for the life of the patient. These long term uses are typically for patients suffering CHF. VAD's need to be clearly distinguished from artificial hearts, which are designed to completely take over cardiac function and generally require the removal of the patient native heart. Among the available blood pumps, the axial and centrifugal blood pumps have received the most interest for use as VAD, because it permits a compact design and can achieve high blood flow rates. Hemolysis tests and animal experiments have proven that the blood pump has an acceptable but a not ideal hemolysis level; thrombus occurred and CFD analysis showed regions of

Corresponding Author: D.H. Hussein, School of Mechanical Engineering, University of Sains Malaysia, Pulau Penang, 14300 Nibong Tebal, Malaysia

reverse flow present in the diffuser, which is not only decreasing the pump's hydrodynamic efficiency. However, increases its overall potential for blood trauma and thrombosis (Yan Zhang *et al*., 2008). One of the crucial challenges for current VAD's is blood trauma including both hemolysis and thrombosis resulting from high shear stress and stagnation effects on as the blood passes through the VAD. Normal human blood contains Red Blood Cells (RBC's), which is the most important element of the blood. Hemolysis is the rupture of the RBC's, which releases hemoglobin to the blood plasma. It is caused by high shear stress from mechanical pumping of the blood. Shear stress has a direct correlation with hemolysis and stagnation has a direct correlation with thrombosis. Both an axial and centrifugal blood pumps are well known in the hydraulic and pneumatic fields. They typically consist of a rotating impeller. Generally, the fluid inlet or suction port feeds fluid to the hub or the center of the impeller. A number of impeller vanes generally project outward from the hub in spiral paths and are supported between shrouds, which together with the vanes, constitute the pumping channels. The impeller is encased in a housing that channels the working fluid from the inlet port to the hub or the inducer, where it is inducted into the pumping channels between the vanes and the shrouds. The axial action of the impeller drives the working fluid outward to a diffuser at the axial and periphery of the impeller (Turton, 1993). The most successful VAD's are designed to be more bio-compatible and induce minimum shear stress on the blood. A number of CFD studies have investigated the effect of geometry on the flow behavior in the pump. There are many applications where a more compact form of the pump is desired. There are also applications, where the shaft and the seals can present operational problems. A well-known example is that of the artificial heart pump where dangerous blood clots can form in the areas where the motor shaft enters the pump housing (Miller *et al*., 1990). In the present study, we focused on the design of a novel cardiac axial blood pump due to its advantages to use as VAD, such as a small size, compact design, magnetically suspended and adequate flow rates. The focus area is shearing stress and blood hemolysis. While, the hydraulic design of the pump delivers appropriate fluctuation against given pressure head, the hemolytic design of the pump is equally important. Blood damage or hemolysis and blood coagulation or thrombosis is two important features of the hemolytic design. A clear understanding of these processes in complex flows in blood handling devices is yet to be formed. In lack of an exact behavior, several models have been proposed in the study that relates the blood damage to the local shear rates in the flow. These models are based on the simple shear flow experiments that measure the time dependent hemolysis at steady shear (Arora *et al*., 1995). Giersiepen *et al*. (1990) developed a correlation for steady shear hemolysis in short time scales relevant to flow in a blood pump based on experimental results. The correlation is (Eq. 1):

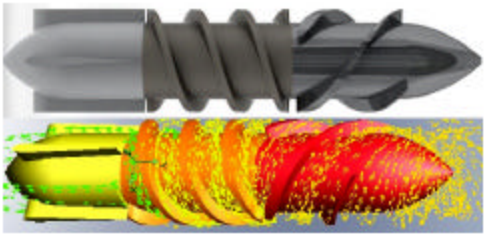

Fig. 1: A 3D top view of the CABP core components

$$\frac{\Delta Hb}{Hb} = 3.62\times10^{-7}\,\sigma^{2.416}\,\Delta t^{0.785}\ (Pa.s) \qquad (1)$$

where:

ΔHb/Hb = Hemolysis index or the ratio of plasma free hemoglobin to the total hemoglobin in the sample (Pa.s)
5H = The shear stress (Pa)
t = Exposure time (sec)

Figure 1 shows the three dimensional top view core components geometry of the novel design of the Cardiac Blood Pump (CABP), it is a device designed to be used as an implantable pump to support the blood circulation in patient who heart is not pumping an adequate cardiac outlet.

MATERIALS AND METHODS

Solid works and COSMOS flow software version 2007 are employed for modeling and simulation of the CABP. The study considers six different rotational speed (from 5000-7000 rpm) clockwise. The aims are to study the flow streamlines behavior, the shear stresses on the fluid, shear stress on the impeller, maximum pressure and the pressure drop of the pump. The simulation have been done under the atmospheric pressure, no gravity, Temperature 37°C, inlet volume flow rate 5 L min^{-1} and the ideal human blood characteristics were identified as working fluid while, titanium applied as a material for all the pump components.

Geometry of the pump: Figure 2 shows 3D top view of the CABP model. The pump has a case and core, the pump core consists of three parts: straighter, impeller and

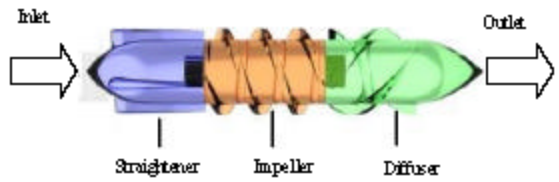

Fig. 2: A 3D top view of the CABP model

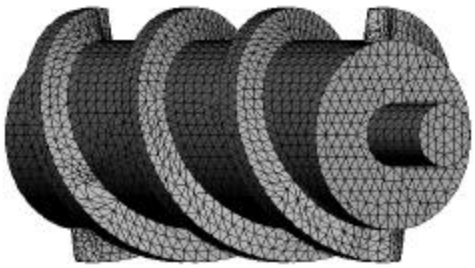

Fig. 3: The mesh form of the pump impeller

diffuser were axially assembled. The impeller has a 30 mm length and 20 mm diameter. It has two curved blades 650° clockwise, the impeller has to move around the axial direction freely. The straighter has 30 mm length and 20.5 mm diameter and it has 4 straight blades. The diffuser has 40 mm length and 20.5 mm diameter and it has three curved blades. The cylindrical case has a circular axial inlet and outlet 20.4 mm diameter. The radial clearance between the impeller and the housing is 0.2 mm. The straighter impeller blades gap junction is 0.5 mm and the impeller diffuser blades gap junction is 1.5 mm. Pressure and shear stress has been detected along 100 mm line through the pump and 0.1 mm distance from the case.

In the future designing research could be use this information in conjunction with experimental data and practical experience. Field testing is mandatory to validate our final design. COSMOS researches help us reduce the time-to-market by reducing but not eliminating field tests.

Meshing: Using fine and suitable mesh lead to get high quality data very close to the real data. Modeling right procedures lead to create a fine and quality mesh. Finite Element Analysis (FEA) provides a dependable numerical technique for analyzing engineering designs. The process starts with the creation of a geometric model. Then, the program subdivides the model into small simple elements connected at common points (nodes). Finite element analysis programs appear at the model as a network of discrete interconnected elements. The Finite Element Method (FEM) predicts the behavior of the model by combining the information obtained from all elements making up the model. The software estimates a global element size for the model considering its volume, surface area and other geometric details. In the present study, meshing generated 3D tetrahedral solid elements and 2D triangular shell elements (Fig. 3).

Shear stress: The main aim of this study is to predict the shear stress on the working fluid applied by the pump components. In addition, the pressure drop through the pump calculated through the pump along a detector line 0.1 mm distance from the inner surface of the case.

Simulation: Specifying boundary conditions and stator walls-at the inlet boundary condition 5 L min^{-1} volume flow rate has been specified relative to rotating frame. At the outlet boundary condition environment pressure is specified as default value. When, we specify a rotating reference frame, it is assumed that all model walls are rotated, with the reference frame's angular velocity, unless we set a specific wall to be stationary. To specify a non-rotating wall, the stator moving wall boundary condition applied to this wall. Specifying, the stator boundary condition is the same as specifying the zero velocity of this wall in the absolute (non-rotating) frame of reference. Also, the stator face must be axisymmetric with respect to the rotation axis. We specified the stator condition at the corresponding walls of the pump's case, which is the inner face of the case exclude the inlet and outlet faces.

RESULTS AND DISCUSSION

Rotational speed and shear stress: Figure 4 shows the shear stress distribution along the pump impeller at different rotational speeds 5000, 5500, 6000, 6500 and 7000 rpm. Therefore in all five cases as the rotational speed increase the shear stress increase too, maximum shear stress occurred at the distance between 20 and 60 mm, where is the location of the rotating part or the pump, which is expected.

Pressure drop and hydraulic pressure gain: The design have to achieve 100 mmHg pressure drop. Pressure drop and hydraulic gain have a direct correlation with rotational speed. From Eq. 2, hydraulic gain can be calculated by dividing the total pressure drop over the outlet dynamic pressure. From Fig. 5, it can be seen as the rotational speed increase the pressure drop also increases. Table 1 shows the pump performance in terms of pressure drop, maximum shear stress and hydraulic gain. From Table 1, at rotational speed of 6500 rpm the pressure drop is 103 mmHg and the hydraulic gain 323, which is very close to the required value of the pressure drop, at 7000 rpm the pressure drop 129 mmHg and hydraulic gain 468, higher

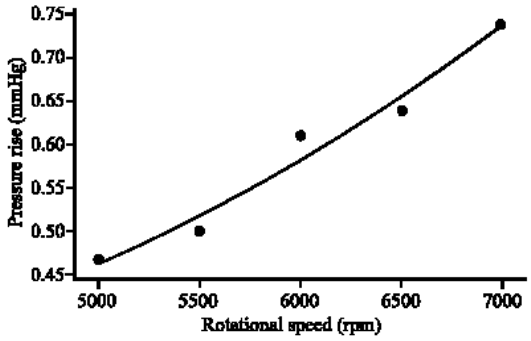

Fig. 4: Maximum shear stress in term of rotational speed

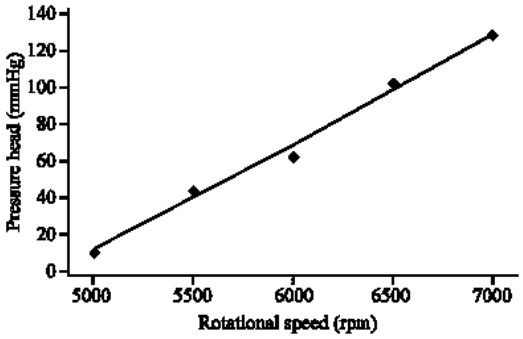

Fig. 5: Pressure rise in term of rotational speed

Table 1: Performance of the pump at different rotational speeds

Rotational speed (rpm)	Max shear stress (mmHg)	Pressure drop (mmHg)	Hydraulic gain (unit less)
5000	0.47	9.5	5.7
5500	0.50	46.0	32.0
6000	0.61	62.0	47.0
6500	0.64	103.0	323.0
7000	0.74	129.0	468.0

pressure drop and hydraulic gain can be achieved, but as the speed increase the maximum shear stress and blood hemolysis also will increase (Eq. 2):

$$HG=\frac{\Delta P}{Pd} \quad (2)$$

where,

HG = Hydraulic pressure gain
ΔP = Pressure drop
Pd = Dynamic pressure at the outlet

Figure 6 shows the pump performance in terms of hydraulic gain and pressure drop, as can be seen the pressure drop has liner behavior and its increased gradually and stable as the rotational speed increased while, the hydraulic pressure gain has a non liner behavior. From the presented results, the rotational speed of 6500 rpm is highly recommended for this design.

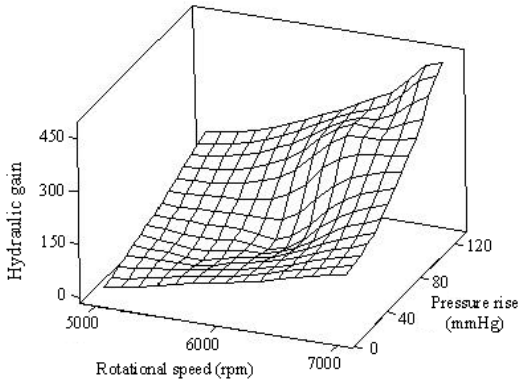

Fig. 6: Hydraulic gain in term of pressure and rotational speed

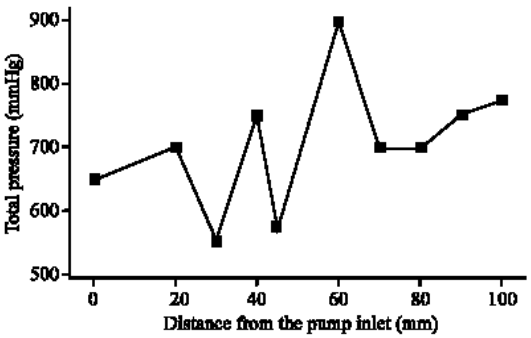

Fig. 7: Pressure distribution inside the pump

Pressure drop: Figure 7 shows the pump pressure distribution at rotational speed of 6500 rpm, as can be seen the inlet total pressure is 656.8 mmHg, at the straighter region from the inlet to 30 mm distance about 650 mmHg, while, there is a pressure drop to 550 mmHg at 35 mm distance. At the impeller region, there are two pressure peaks first one is 700 mmHg at 40 mm, while second one is the maximum pressure peak 900 mmHg at 60 mm distance, located exactly at 1.5 mm gap between the impeller and diffuser blades, which is a very attractive point for further research work to optimize the gap. From 60-80 mm the pressure decreased dramatically to 675 mmHg then at the outlet the pressure increased gradually to reach 760.3 mmHg. Taken as a whole, the total pressure drop from the inlet to the outlet is 103.5 mmHg. Which is optimal value to realize the best pump concert.

Critical areas of shear stress on the fluid: At rotational speed of 6500 rpm the shear stress detected through the pump, because at the speed the pump pressure drop is 103.5, which are the best value. At the straighter region from the inlet to 30 mm distance, the shear stress has the

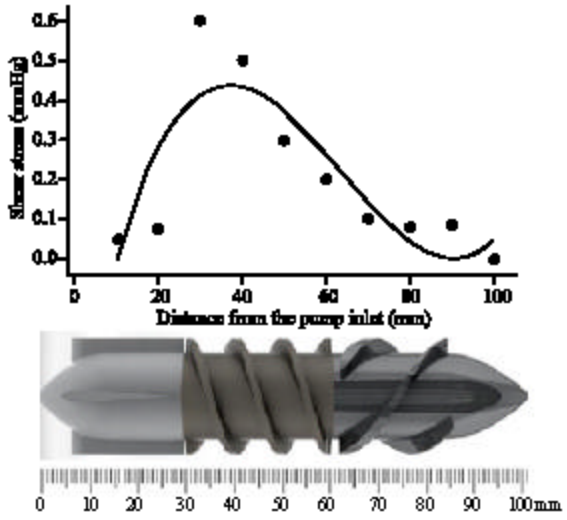

Fig. 8: Sheare stress distribution along the pump impeller

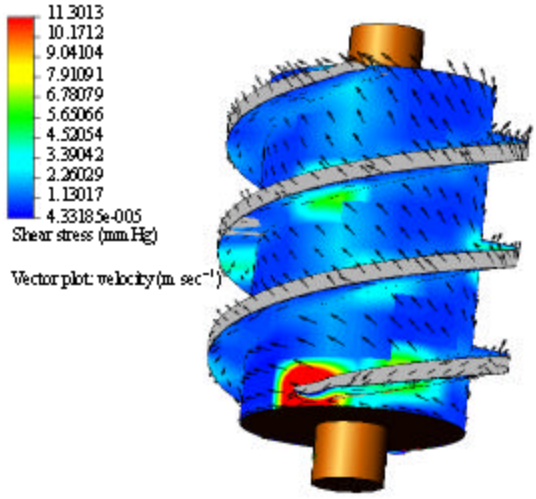

Fig. 9: Shear stress distribution and velocity vectors on the pump impeller

lowest value about 0.02 mmHg, which is expected due to stationary blades of the straighter. At the impeller region from 30-40 mm, the shear stress increased dramatically to reach the maximum peak 0.65 mmHg at 40 mm about the first quarter of the impeller, this is due to the transfer junction from flow within stationary blades of the straighter to the flow within movable blades of the impeller. From 40-70 mm the shear stress dropped gradually from 0.65-0.07 mmHg during the rest of the impeller distance. From 70-80 mm, shear stress increased to 0.1 mmHg because at the first half of the diffuser. Near the outlet from 90-100 mm the shear stress dropped again to be at the lowest value 0.02 and very similar with its value at the inlet. Figure 8 shows the shear stress distribution along the pump impeller at 6500 rpm.

Shear stress on the pump impeller and the velocity vectors: To avoid the mechanical failure, shear stress on the impeller is one of the crucial design concerns, Fig. 9 shows the shear stress distribution and velocity vectors on the pump impeller at the rotational speed 6 K rpm, as can be seen most of the body area under shear stress about 1.13 mmHg the blue areas of the graph. Even as, the base area of the impeller blades under shear stress about 5.6 mmHg the light green areas. Therefore, the maximum shear stress about 11 mmHg applicable to the pump impeller located exactly at the base areas of the proximal edges of both impeller blades about 31 mm distance from the pump inlet. The velocity vectors run toward the diffuser on the perpendicular direction to the blades upper side plane.

Flow streamlines: Flow streamlines are lines where, the flow velocity vector is tangent to that line at any point on the line. Also, streamlines defined at a single instant in a flow do not intersect. Because a fluid particle cannot have two different velocities at the same point. Because two particles cannot be present at the same location at the same instance of time. However, to display a streamline, we have to specify any streamline point, which is a point through, which the trajectory passes and the streamline direction with respect to this point. If we specify forward direction then the streamline is displayed starting from this point. If backward direction is selected, the streamline is displayed ending at this point. In the present study, we specified both directions to allow us to display a flow streamline from the beginning to the end, passing through the selected point. Figure 10a shows the flow streamlines are passing through the pump and around its interior components: straighter, impeller and diffuser. Most of the turbulent flow and shear stress may be expected at the inner components gape at junctions and the interaction between the movable and stationary parts or walls. In the present study, the impeller is the only movable part. When streamlines enter the pump inlet at the straighter region all the flow streamlines run together parallel the straighter blades and case wall. Figure 10b shows enlargement three dimensional view of the flow streamlines around the impeller. The flow stream lines can be seen more clearly in Fig. 10c as can be seen most of the streamlines run forwardly and divided into two main groups as we named them: γ-group and β-group. γ-group runs in the clearance between the case wall and the impeller blades. The fluid particles in this case take the shortest ways to pass through the pump. Therefore, γ-group will be applied for the shortest time exposure. Based on this γ-group will be applicable for less shear stress. While, β-group runs in the helical channels of the upper and lower blade faces and parallel to the impeller blades. The fluid particles in this case take long ways to

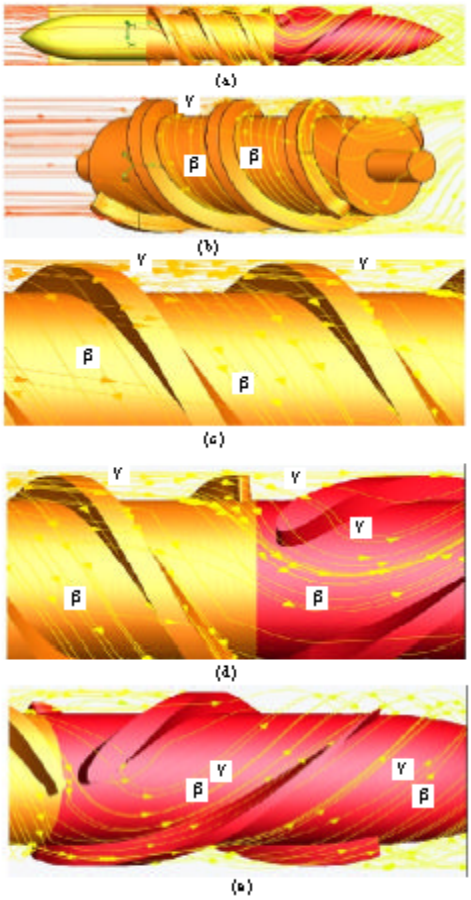

Fig. 10: Flow stream lines

pass through the pump. However, in fact we have to minimize the flow of γ-group streamlines in the parallel direction to increase the pump efficiency this can be done by minimize the clearance between the impeller blades and the case. While, β-group will be applied for longest time exposure, based on this even if the shear stress along the stream lines of both groups the same value, β-group will be applicable for time exposure longer than γ-group. Figure 10d and e show both γ-group and β-group of the flow streamlines passing the diffuser region. At the first quarter of the diffuser, both groups become together in the same direction. The flow direction of all streamlines become parallel to the stationary diffuser blades tell the streamlines leave the pump outlet.

Outlet pressure: Located at the diffuser region shown in Fig. 11a, the fluid exit from the pump outlet in form of unit axial vortex.

Maximum pressure: Located between the impeller and the diffuser region, shown in Fig. 11b where, the fluid leaves the impeller region to the diffuser.

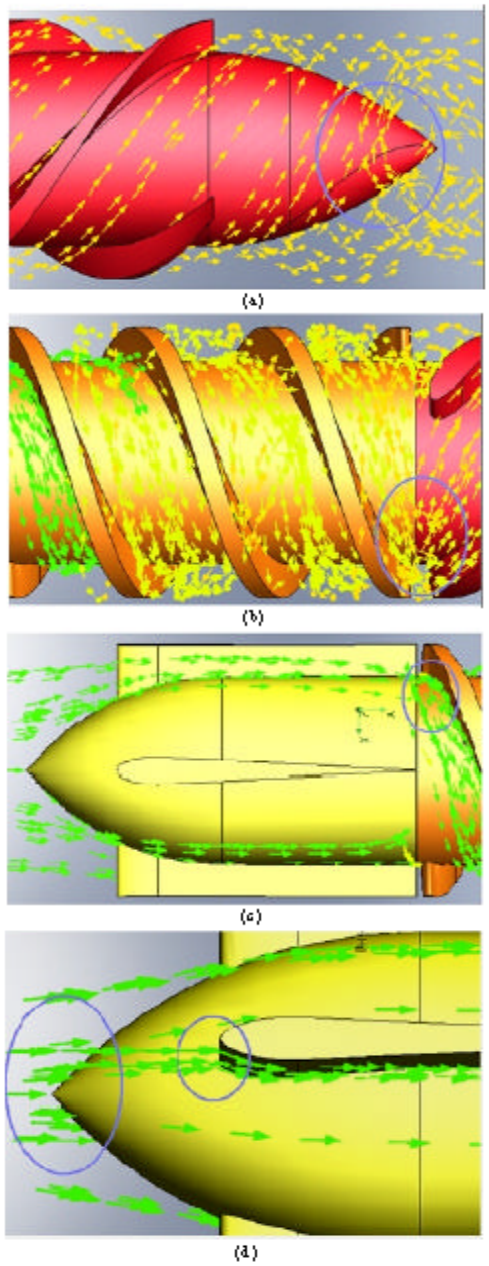

Fig. 11: Critical fluid flow areas. a) Outlet pressure, b) Maximum pressure, c) Maximum shear pressure and d) Stagnation point

Maximum shear stress: Located between the straighter and the impeller region shown in Fig. 11c at the beginning of the suction region.

Stagnation: Located at the front tips of the straighter body and straighter. At these points shear stress and velocity expected to be minimum but stagnation in the blood pumps not desired because, its increase of the blood thrombosis (16).

CONCLUSION

The maximum pressure peak 900 mmHg on the fluid located at 60 mm distance, located exactly at a gap between the impeller and diffuser blades. Shear stress and maximum pressure on the fluid located reach their highest values around the impeller about 35-75 mm distance from the pump inlet. Maximum shear stress, pressure drop and shear stress on the impeller have a direct correlation with rotational speed. Maximum shear stress on the impeller occurs at the base of the proximal edges of the impeller blades about 31 mm distance from the pump inlet. Flow streamlines behave differently as 2 groups in the impeller region about 30-60 mm distance from the pump inlet due to the clearance between the blades and the case of the pump.

Current research is undergoing to measure the performance of the scale model of the pump. Particle imaging velocimetry will be used to verify the flow characteristics. The current design will undergo optimization of the impeller blade, clearance, angular curvature and blades thickness.

REFERENCES

Arora, D. and C. Bludszuweit *et al.*, 1995. Three-dimensional numerical prediction of GYRO blood pump: Hemolysis and rate of hemolysis along the particle traces. Third MIT Conference on Computational Fluid and Solid Mechanics 581 stress loading of blood particles in a centrifugal pump. Artificial Organs, 19: 590-596.

Giersiepen, M., L.J. Wurzinger, R. Opitz, H. Reul, 1990. Estimation of shear stress-related blood damage in heart valve prostheses-in vitro comparison of 25 aortic valves. Int. J. Artificial Organs, 13: 300-306.

Hafez, M.M., 2003. Numerical simulation of incompressible flows. World Scientific, pp: 680. ISBN: 981-238-317-4.

Hussein, D.H. and H. Gitano-Briggs, 2008. Outlet optimization of the centrifugal blood pump. J. Eng. Applied Sci., 3 (9): 702-707.

Miller, G.E., B.D. Etter and J.M. Dorsi, 1990. A multiple disk centrifugal pump as a blood flow device. IEEE. J. Trans. Biomed. Eng., 37 (2): 157-163.

Noon, G.P., D. Morley, S. Irwin and R. Benkowski, 2000. Development and clinical application of the micro-med debakey VAD. Curr. Opinion Cardiol., 15: 166-171.

Tetsuzo, A., 1975. Artificial Heart Total Replacement and Partial Support. 1st Edn. Igaku Shoin, American Elsevier. ISBN: 0-444-16705-6.

Turton, R.K., 1993. An introductory guide to pumps and pumping systems. Mechanical Engineering Publication, London, UK. DOI: 10.1109/TMECH.2006. 882984.

Yan Zhang, Zhao Zhan, Xing-ming Gui, Han-Song Sun, Hao Zhang, Zhe Zheng, Jian-Ye Zhou, Xiao-Dong Zhu, Guo-rong Li, Sheng-Shou Hu and Dong-hai Jin, 2008. Biomedical engineering. J. Am. Soc. Artificial Internal Organs, 54 (2): 150-155. DOI: 10.1097/MAT. 0b013e318164137f.